THE ROYAL SOCIETY

doi 10.1098/rspb.2001.1794

Limitation of *Trypanosoma brucei* parasitaemia results from density-dependent parasite differentiation and parasite killing by the host immune response

Kevin M. Tyler[1*,2], Paul G. Higgs[2], Keith R. Matthews[2] and Keith Gull[2]

[1]*Department of Pathology, Northwestern University Medical School, 303 E. Chicago Avenue, Chicago, IL 60611, USA*
[2]*School of Biological Sciences, University of Manchester, Stopford Building, Oxford Road, Manchester M13 9PT, UK*

In the bloodstream of its mammalian host, the 'slender' form of *Trypanosoma brucei* replicates extracellularly, producing a parasitaemia. At high density, the level of parasitaemia is limited at a sublethal level by differentiation to the non-replicative 'stumpy' form and by the host immune response. Here, we derive continuous time equations to model the time-course, cell types and level of trypanosome parasitaemia, and compare the best fits with experimental data. The best fits that were obtained favour a model in which both density-dependent trypanosome differentiation and host immune response have a role in limiting the increase of parasites, much poorer fits being obtained when differentiation and immune response are considered independently of one another. Best fits also favour a model in which the slender-to-stumpy differentiation progresses in a manner that is essentially independent of the cell cycle. Finally, these models also make the prediction that the density-dependent trypanosome differentiation mechanism can give rise to oscillations in parasitaemia level. These oscillations are independent of the immune system and are not due to antigenic variation.

Keywords: trypanosomiasis; mathematical model; sleeping sickness

1. INTRODUCTION

Trypanosoma brucei maintains a chronic parasitaemia in a wide range of mammalian hosts. The mechanisms by which this is achieved are necessarily complex (Barry & Turner 1991). This complexity stems from the balance of trypanosome proliferation, differentiation and cell death. Proliferation must be great enough to achieve transmission and to avoid clearance, but not so great as to cause the death of the host. This balance must also be able to compensate for parasite clearance by the immune system and for the emergence of new variant antigenic types (VATs) by switching of the variant surface glycoprotein (VSG) coat of the trypanosome—a process known as antigenic variation.

Even in the absence of an immune response, differentiation to the 'stumpy' form will limit trypanosome growth, causing the level of parasitaemia to plateau at a sublethal level in mice for up to 72 h (Balber 1972). By comparison, monomorphic lines, which do not differentiate to the stumpy form in mice, invariably reach a lethal parasitaemia even in immunocompetent murine hosts. This is regardless of their mean doubling time, which might be longer than that of pleomorphic strains (Turner *et al.* 1995).

In immunocompromised hosts, the level at which the primary parasitaemic peak is reached is host specific, showing variation even within species (Seed & Sechelski 1988). This observation implies that host factors that are not solely lymphocyte derived (such as antibody), interact with the trypanosomes and, thus, affect differentiation to the stumpy form. The potential importance of the host in mediating the slender-to-stumpy differentiation is reinforced by the observation that strains that are monomorphic in rodents are pleomorphic when introduced into other mammals (Black *et al.* 1983).

Parasite clearance in an immunocompetent host almost exclusively reflects the onset of a humoral immune response. The effectiveness of this response to any one VAT is apparently host specific (reviewed in Barry & Turner 1991). It might have a strong genetic component that varies markedly even between related mouse strains (Seed & Sechelski 1995). Animals that mount effective, rapid immune responses markedly limit parasitaemia; growth curves obtained from such animals are often of the classically undulating sort, normally prolonged and sometimes self-curing. Other animals, however, apparently mount a slower response that is often less effective at ameliorating the parasitaemia. The parasitaemia of these animals is limited by differentiation to the stumpy form during the delay, until the immune response is able to act (reviewed in Black *et al.* 1985). Slender forms are more susceptible to complement-mediated lysis than stumpy forms (McLintock *et al.* 1993) and so are cleared preferentially by the immune response. Stumpy forms, however, have also been suggested to elicit a stronger immune response than slender forms (Sendashonga & Black 1982).

Differentiation has been found to be a function of trypanosome density (Seed & Sechelski 1989) and this has been confirmed by recent reports of a stumpy induction factor (Hesse *et al.* 1995; Vassella & Boshart 1996; Vassella *et al.* 1997; reviewed in Matthews 1999). We sought to further examine density-dependent models to determine whether our experimental results could be adequately explained by density-dependent trypanosome

*Author for correspondence (k-tyler@northwestern.edu).

differentiation. In doing so, a simulation of the primary parasitaemia, which assumes the rate of differentiation to be a function of parasite density, was developed.

2. MATERIAL AND METHODS

(a) *Trypanosomes and mice*

All studies used immunocompetent adult female BALB/c and CD1 mice that were inoculated with either pleomorphic GUP 2962 (McLintock *et al.* 1990) or monomorphic GUP 2965 (Barry *et al.* 1985) (kind gifts of Dr C. M. R. Turner, University of Glasgow, UK). The VAT of both these lines was GUTat 7.2., and both lines were derived from the EATRO 2340 stabilate of *Trypanosoma brucei rhodesiense*.

(b) *Growth of trypanosomes in mice*

Mice were inoculated intraperitoneally, with *ca.* 1×10^6 slender trypanosomes from a frozen stock suspended in 0.3 ml of PSG (488.8 mg l^{-1} NaH_2PO_4, 2.55 g l^{-1} NaCl, 8.08 g l^{-1} Na_2HPO_4, 15 g l^{-1} D-glucose; pH 7.8). Parasitaemias were monitored from the third day after infection using an improved Neubauer haemocytometer (Brightline, Buffalo, NY, USA). Blood smears were made from the same tail bleeds as those used for bloodstream counts, allowing assays by morphological and NAD diaphorase criteria to be related to parasitaemia at each time point.

(c) *NAD diaphorase assay*

Blood smears were fixed for 5 min, with 2.5% (v/v) electron microscopy grade glutaraldehyde (TAAB) in PBS (pH 7.4). Slides were then rinsed in distilled water and incubated in a humid chamber for 2 h with freshly prepared reaction mixture that contained 1.3 mg ml^{-1} of the reduced form of β-nicotinamide adenosine dinucleotide (NADH) disodium salt and 0.3 mg ml^{-1} nitrotetrazolium blue, dissolved in PBS (pH 7.4). Slides were stained with 1 μg ml^{-1} DAPI (4′,6-diamidino-2-phenylindole dihydrochloride) for 30 s, rinsed with distilled water, mounted with Vectashield (Vector Laboratories, Peterborough, UK) and sealed with nail varnish.

3. RESULTS AND DISCUSSION

In developing a model system for growth and differentiation of bloodstream form trypanosomes, two widely available inbred strains of mice were initially tested: CD1 and BALB/c. Representative growth curves (selected from a large number of very similar datasets) are shown in figure 1*a*,*b*. The prepatent period of infection with the pleomorphic line GUP 2962 varied by up to 12 h in mice, regardless of whether BALB/c or CD1 was used. In comparing the growth curves of GUP 2962 in CD1 with those in BALB/c mice, initial growth seemed similar; however, it seemed that by 80 h the infection was being controlled in CD1 mice—the level of parasitaemia dipping long before the peak reached by the BALB/c mice. Monomorphic GUP 2965 was also tested in the mice (figure 1*c*). Extremely high parasitaemias were reached and in neither host was there an obvious reduction in growth rate or evidence of morphological differentiation to stumpy forms.

These data highlight the variability in the parasitaemic profiles obtained with different hosts or trypanosome lines. Ideally, we would like to be able to accommodate

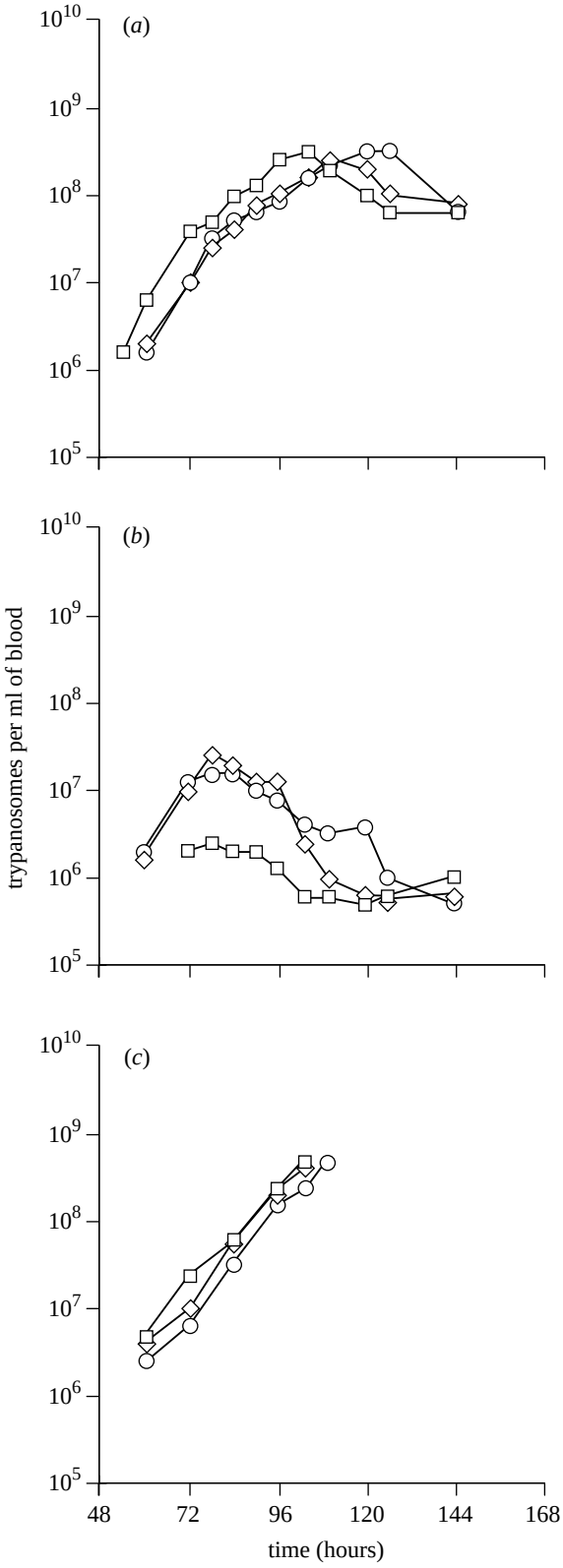

Figure 1. Growth of pleomorphic (GUP 2962) and monomorphic (GUP 2965) lines of *Trypanosoma brucei rhodesiense* in immunocompetent inbred lines of mice. The data are presented in triplicate sets. The inoculations of BALB/c mice and CD1 mice with GUP 2962 (*a* and *b*, respectively) were done in parallel as a single experiment. Inoculation of BALB/c mice with GUP 2965 (*c*) was carried out as a single but separate experiment.

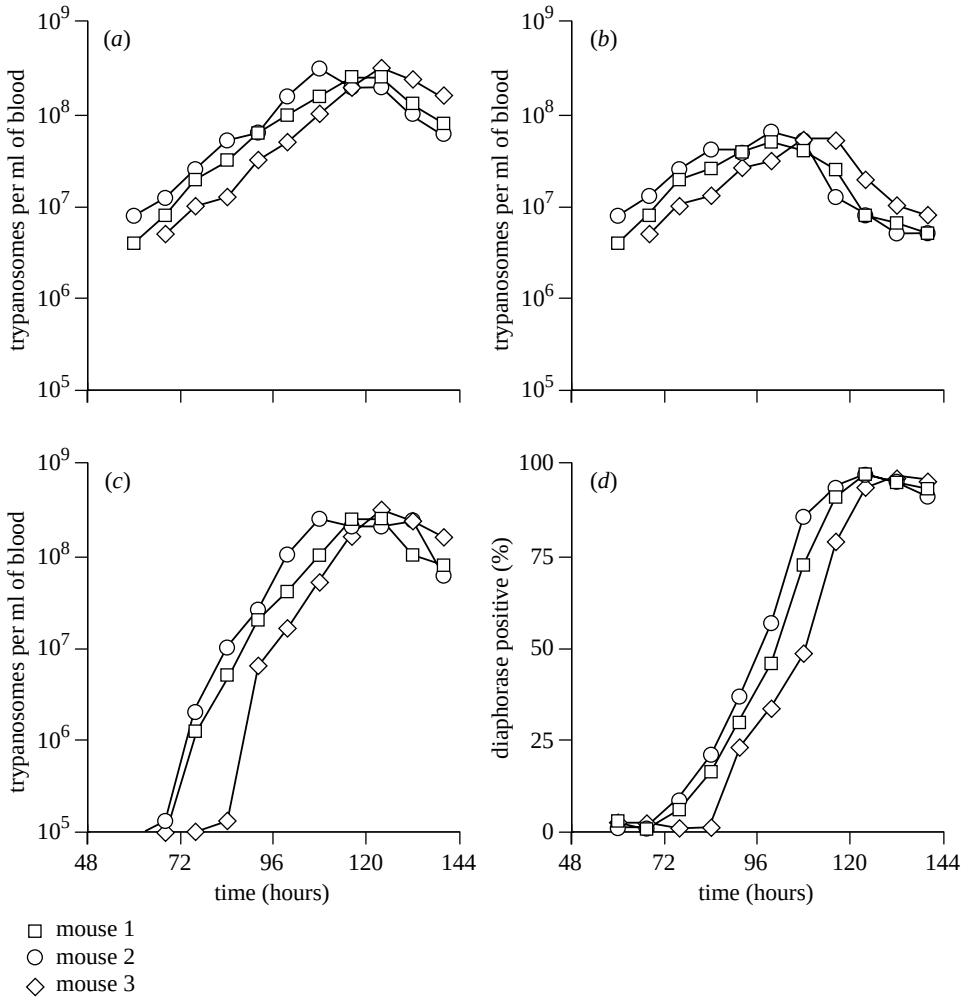

Figure 2. Acquisition of diaphorase activity as a marker of the slender-to-stumpy differentiation during the primary parasitaemia of GUP 2962 in a BALB/c mouse. This single experiment was carried out in triplicate. At each 8 h time point, blood smears were prepared that were then assayed cytochemically for diaphorase activity. When a characteristic deposit of formazan along the mitochondrion was observed, trypanosomes were scored as 'diaphorase positive'. One thousand trypanosomes were assayed at each time point for each mouse. (*a*) Total, (*b*) diaphorase negative, (*c*) diaphorase positive, and (*d*) percentage diaphorase positive.

all parasitaemic profiles in a single mathematical model simply by variation of key parameters that are defined experimentally. The rate of differentiation from the proliferative slender to non-proliferative stumpy form is one such parameter that can be investigated. This differentiation was most tractable in BALB/c mice, which gave the most consistent growth curves. Consequently, the parasitaemia in BALB/c mice was further assessed using the cytochemical diaphorase assay (figure 2), which provides a simple method for discriminating between proliferative (slender, diaphorase negative) and non-proliferative (intermediate and stumpy, diaphorase positive) forms (Vickerman 1965; Tyler *et al.* 1997).

To follow differentiation, tail bleeds were taken from each mouse at each time point shown in figure 2, allowing measurement of parasitaemia and preparation of blood smears. The diaphorase assay was then conducted on the blood smears and assessed using light microscopy. One thousand trypanosomes were assessed for each mouse at each time point, even though at low parasite densities this typically involved the examination of more than one slide.

At low parasitaemia, less than 10% of trypanosomes were diaphorase positive. It is worth noting that even at very low parasitaemia there were at least a few diaphorase-positive forms with clearly stumpy morphology. During logarithmic growth, the proportion of diaphorase-positive trypanosomes increased steadily. By the time of the parasitaemic peak, more than 75% of trypanosomes were diaphorase positive, which increased to more than 95% after the peak, *ca.* 5 days post-infection (figure 2*d*).

Having characterized a reproducible system for a rodent primary parasitaemia, we sought to emulate it using a mathematical model. Density-dependent arithmetic simulations of the primary parasitaemia can show close fits to observed data (Seed & Black 1997, 1999; Tyler 1998), indicating that a density-dependent model can emulate many aspects of experimental datasets. Indeed, it highlights the difficulty that a model based on differentiation as an intrinsic function of growth has in explaining the observation that the number of proliferative forms first increases and then decreases, even in immunosuppressed models. This is because the number of proliferating forms increases throughout if the rate of

differentiation is less than 50% per generation, whereas if the differentiation rate is more than 50% the number of proliferating forms falls throughout.

Introduction of new parameters and variation of parameters to fit theory to experimental data is cumbersome using arithmetic simulations. We therefore devised continuous time equations from arithmetic precepts for use in computer modelling of trypanosome parasitaemias.

(a) *A mathematical model of parasitaemia limited by trypanosome differentiation*

In this section, we consider mathematical modelling of the slender-to-stumpy transition using differential equations to describe the rate of change of the total parasite density with time. We will begin with the model proposed by Turner *et al.* (1995):

$$\mathrm{d}X/\mathrm{d}t = (r - f)X(t), \tag{3.1a}$$

$$\mathrm{d}Y/\mathrm{d}t = fX(t) - mY(t). \tag{3.1b}$$

Here, $X(t)$ is the concentration of slender cells at time t, and $Y(t)$ is the concentration of stumpy cells. The rate of division of slender cells is r, the rate of differentiation of slender-to-stumpy cells is f, and the mortality rate of stumpy cells is m. Turner *et al.* (1995) studied these equations under the assumption that the differentiation rate f is constant. To modify this model by introducing density-dependent trypanosome differentiation, the simplest assumption is that differentiation rate is proportional to total trypanosome concentration $T(t) = X(t) + Y(t)$, i.e.

$$f = f_0 T(t), \tag{3.2}$$

where f_0 is a constant. We have previously shown cytologically that most phenotypic change takes place after G_1/G_0 arrest in all cells (Tyler *et al.* 1997). Commitment to and onset of differentiation, however, occurs before cell-cycle arrest in at least some cells and can be discerned as small but tell-tale changes in key marker proteins and morphological parameters (Tyler *et al.* 1997). The model above supposes that cell division and differentiation are independent events. We will consider an alternative scenario later in this paper (§ 3b, model C) that is consistent with this cytological data, in which a heterogenous differentiation division is an obligatory part of the differentiation pathway. We will refer to the model defined by equations (3.1a), (3.1b) and (3.2) as model A in this paper.

The curves $X(t)$, $Y(t)$ and $T(t)$ were obtained for each trial set of parameters using the standard fourth-order Runge–Kutta method for ordinary differential equations (described in Press *et al.* 1992), using a step length $\mathrm{d}t = 1\,\mathrm{h}$. As initial conditions, we set $X(t) = X_0$ and $Y(t) = 0$. The solution therefore depends on four parameters: r, f_0, m and X_0. The parameter set was chosen to most closely fit the data points by minimizing the root-mean-square (rms) error per data point, S, defined by

$$S^2 = \frac{1}{3N}\sum_{i=1}^{N}\left((\ln X_{\mathrm{obs}}(t_i) - \ln X_{\mathrm{th}}(t_i))^2 + (\ln Y_{\mathrm{obs}}(t_i) - \ln Y_{\mathrm{th}}(t_i))^2 + (\ln T_{\mathrm{obs}}(t_i) - \ln T_{\mathrm{th}}(t_i))^2\right). \tag{3.3}$$

N is the number of measured data points on each curve, hence there are $3N$ points in total. The time of measurement of the ith point is t_i. Subscript 'obs' denotes observed experimental data points, and subscript 'th' denotes theoretical values obtained from numerical solution of the equations. We fitted logarithms of the concentrations because the data points vary over several orders of magnitude. To obtain the optimal parameter set, we made an initial estimate of the parameters, then proceeded by making small changes to parameter values until no further reduction in S could be obtained—checking that the same final solution resulted from different starting points.

For the BALB/c mice with GUP 2962, four datasets were used (experimental curves for three of these are shown in figure 2). The best-fitting parameters for these datasets with model A are shown in table 1. The estimate of the rate of division does not differ much between mice, with the mean value being $r = 0.11\,\mathrm{h}^{-1}$, which corresponds to a doubling time of $\ln 2/r = 6.3\,\mathrm{h}$. The values of f_0 are all *ca.* $1 \times 10^{-9}\,\mathrm{ml\,h}^{-1}$. To examine this further, we might calculate the trypanosome concentration at which the differentiation rate $f = f_0 T$ becomes equal to r. Using the figures for mouse 1, we obtain $T = r/f_0 = 9 \times 10^7\,\mathrm{ml}^{-1}$. Thus, the parasitaemia curves begin to level off substantially when T rises above this value. The values of X_0 differ much more between the mice, presumably reflecting differences in the ability of the founder population to establish infection and enter exponential growth (the measured curves in figure 2 seem to differ principally by sliding along the time axis). The variation in the estimates of m might reflect true variation between mortality rates in the different mice; however, we feel that these figures should be treated with caution as this parameter is not very well constrained by the data and this model does not account for immune killing. Interestingly though, values obtained for m are of the order of previous experimentally derived estimates (Hamm *et al.* 1990; Turner *et al.* 1995).

Figure 3 shows the theoretical fit to the mouse 1 data, showing that the model is correct for the qualitative behaviour. There is an initial exponential growth period, during which almost all trypanosomes are diaphorase-negative, slender forms. The differentiation rate becomes large at *ca.* 96 h, so that the slender curve starts to fall and diaphorase-positive parasite density becomes higher than diaphorase-negative parasite density. At *ca.* 120 h, the diaphorase-positive parasite density reaches a maximum and starts to fall. In the latter part of the infection, almost all trypanosomes are diaphorase positive. It seems that the maximum in the diaphorase-positive and the total trypanosome concentrations is less sharp in the theoretical curves than in curves derived from the experimental values, and the fall off after the maximum is less rapid for the theoretical curves. If other parameter values are chosen, this maximum can be sharpened, but this reduces the quality of fit overall. The curves shown minimize the rms error S over the whole data. In the following section, we will consider modifications to this model in an attempt to improve the fit.

An interesting observation is made if the theoretical curves are extrapolated (figure 4). Oscillations are seen in concentrations of both diaphorase-negative and diaphorase-positive forms that gradually decrease in amplitude. Oscillatory parasitaemia levels in trypanosome infections are well known. The usual explanation

Table 1. Best-fit parameters for model A to data from four BALB/c mice infected with GUP 2962.

	$r\,(\mathrm{h}^{-1})$	$f_0\,(\mathrm{ml\,h}^{-1})$	$m(\mathrm{h}^{-1})$	$X_0(\mathrm{ml}^{-1})$	S
mouse 1	0.11	1.2×10^{-9}	0.012	3.91×10^{3}	0.374
mouse 2	0.12	1.1×10^{-9}	0.017	2.6×10^{3}	0.446
mouse 3	0.11	9.3×10^{-10}	0.000	2.0×10^{3}	0.540
mouse 4	0.10	1.1×10^{-9}	0.020	2.8×10^{4}	0.373

for these is that antigenic variation creates a succession of parasites with different VSG coats, each of which is destroyed in turn by the immune response. Models of this process have been studied previously by Agur *et al.* (1989), Antia *et al.* (1996) and Frank (1999). Our model takes no account of the immune system or of antigenic variation, but oscillatory behaviour is still seen, because when total trypanosome concentration is high, the differentiation rate is high, which leads to a decrease in slender cell concentration and a rise in stumpy forms. However, when trypanosome concentration falls owing to death of the stumpy form, the differentiation rate falls and the slender cell replication increases. We wish to emphasize that although antigenic variation is an important factor in natural infections, it is not the sole source of oscillatory parasitaemia levels.

Seed & Black (1997) did show oscillations in slender cell concentration, but this was caused by an *ad hoc* reduction of differentiation rate to 20% at a particular point. In our model, these oscillations emerge naturally because the differentiation rate falls gradually when total trypanosome concentration starts to fall. Seed & Black's (1997) model does not have a parameter equivalent to our m, the mortality rate of stumpy cells. Therefore, stumpy cells do not decrease in their model after the maximum value is reached. We felt that this parameter was necessary to explain our data. If, in our model, we set $m=0$, diaphorase-positive forms rise to a maximum and then remain constant. As total trypanosome concentration remains high, differentiation rate does not fall, and therefore diaphorase-negative trypanosomes continue to decrease steadily at later times without oscillating.

(b) *More complex mathematical models*

We tried several different models that include additional features not present in model A, in an attempt to increase the accuracy of fit to the data. One factor considered was that when a slender cell becomes committed to differentiation, it might take time to become diaphorase-positive. To account for this, we considered model B, defined by the following equations:

$$\mathrm{d}X/\mathrm{d}t = (r-f)X(t), \tag{3.4a}$$

$$\mathrm{d}E/\mathrm{d}t = fX(t) - aE(t), \tag{3.4b}$$

$$\mathrm{d}Y/\mathrm{d}t = aE(t) - mY(t). \tag{3.4c}$$

In this case, $E(t)$ represents a population of trypanosomes that have exited the cell cycle and are non-proliferative, but are still diaphorase-negative. The E trypanosomes become diaphorase-positive at a rate a. The total trypanosome concentration is $T=X+E+Y$, and the differentiation rate is assumed to be proportional to T, as in

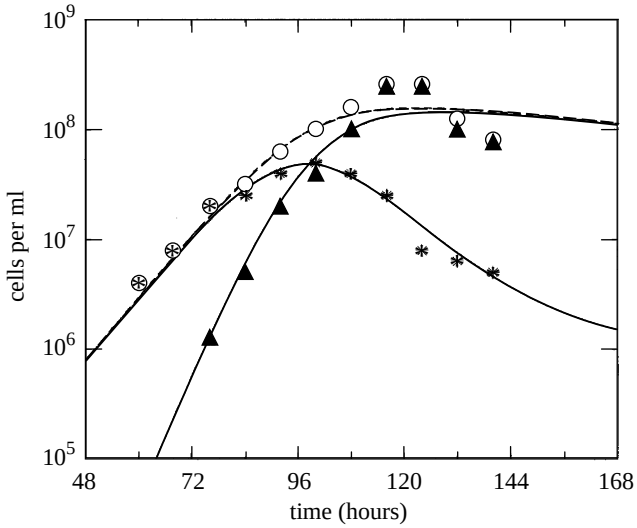

Figure 3. Fitting model A to the BALB/c mouse with GUP 2962. The example shown is mouse 1 in figure 2 and in table 1. Circles, total trypanosome concentration; triangles, diaphorase-positive trypanosomes fitted to the stumpy theoretical curve; stars, diaphorase-negative trypanosomes fitted to the slender theoretical curve.

equation (3.2). The mouse data were fitted to model B using the same method as before. In this case, the measured points for diaphorase-negative trypanosomes were fitted to the sum $X(t)+E(t)$ calculated from theory, whereas diaphorase-positive measurements were fitted to $Y(t)$ as before.

As an example of the fit of this and subsequent models, we will consider mouse 1 only. The optimal parameter values were found to be $r=0.11\,\mathrm{h}^{-1}$; $f_0=1.2\times10^{-9}\,\mathrm{ml\,h}^{-1}$; $a=0.074\,\mathrm{h}^{-1}$; $m=0.010\,\mathrm{h}^{-1}$; and $T_0=4.0\times10^{4}\,\mathrm{ml}^{-1}$. However, the error was $S=0.369$, which is only slightly lower than the corresponding error for mouse 1 with model A (0.374). Visually, the curves for model B are virtually indistinguishable from model A. The problem with model B is that we have introduced an extra quantity, $E(t)$, for which there is no independent experimental measurement. For this reason, it is difficult to determine the model parameters with precision: a and m can vary without making much difference to the fit. Thus, model B does not make a significant improvement to model A.

We will now consider a scenario in which division is an obligatory part of the slender-to-stumpy differentiation pathway. In this case, a slender cell becomes committed to differentiation before division and a differentiating slender cell divides for the final time to produce two stumpy cells. The total rate of cell division is r, as before. Let D be the fraction of cell divisions that lead to stumpy cells. The rate of production of stumpy cells is therefore $2Dr$ (because two stumpy forms are produced for each division). The fraction of proliferative divisions (producing two slender cells) is $1-D$. A division of this type increases the number of slender cells by 1, whereas a differentiation division decreases the number of slender cells by 1. The rate of change of slender cells is therefore $+(1-D)r-Dr=(1-2D)r$. This gives us model C, defined by the equations

$$\mathrm{d}X/\mathrm{d}t = (1-2D)rX(t), \tag{3.5a}$$

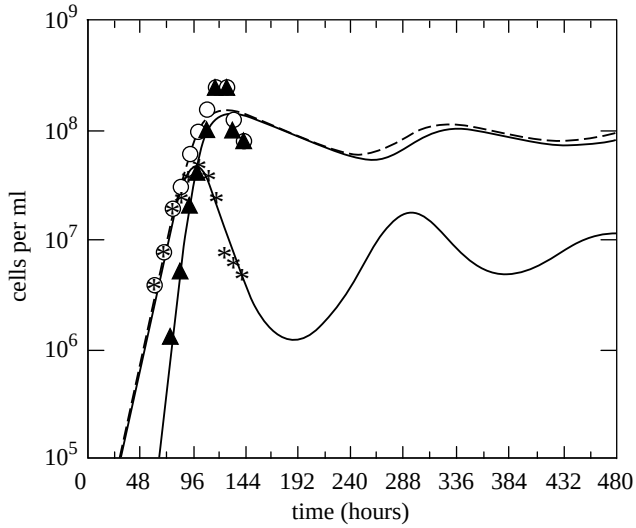

Figure 4. Continuation of the theoretical curves for model A to later times shows that oscillations in trypanosome concentration are to be expected. The parameter values are the same as in figure 3.

$$\mathrm{d}Y/\mathrm{d}t = 2DrX(t) - mY(t). \tag{3.5b}$$

We also need to specify the way that D depends on the total trypanosome concentration T. We will use a function such that $D=0$ for $T=0$, and D increases to 1 for very large T,

$$D = T/(T_1 + T). \tag{3.6}$$

The parameter T_1 is the trypanosome concentration at which half the cell divisions lead to differentiation.

The best-fit parameters for mouse 1 with model C were $r=0.131\,\mathrm{h}^{-1}$; $m=0.0036\,\mathrm{h}^{-1}$; $T_0=7.7\times10^2\,\mathrm{ml}^{-1}$; and $T_1=8.4\times10^7\,\mathrm{ml}^{-1}$. The rms error was $S=0.535$, which is substantially worse than model A. We have previously shown that during cell division some trypanosomes undergo a differentiation division that produces at least one stumpy form and that is heterologous to preceding proliferative divisions (Tyler *et al.* 1997). We have gone on to suggest that both the products of this division become stumpy forms (Tyler *et al.* 2001); however, we have previously been unable to determine whether this cell division is an obligatory part of the slender-to-stumpy differentiation pathway or whether differentiation occurs in a manner that is essentially independent of the cell cycle. Although the fits obtained here favour the latter hypothesis, there are relatively large uncertainties in experimental measurements, which prevent us considering this result as conclusive.

Other functions of T could be proposed instead of the simple one in equation (3.6). For example, D might tend to a maximum that is less than 1 at high T, or D might be non-zero even when T is very low. Alternatively, we could propose a sigmoidal function of T, rather than the linear increase followed by saturation given by equation (3.6). We have tried several of these variants, but all involve the addition of extra parameters that cannot be precisely determined from the data. In the absence of additional experimental data, we conclude that equation (3.6) is as good as any.

In all the models so far, the differentiation rate has been assumed to be a function of the total trypanosome concentration. This raises the question of how individual trypanosomes sense the trypanosome population density. Reuner *et al.* (1997) have argued that trypanosomes release a signal molecule, termed the stumpy induction factor (SIF). The SIF builds up in the bloodstream and initiates the differentiation mechanism when trypanosomes sense its presence in high concentrations. Although the experimental evidence indicates that there is a SIF molecule, it is not yet known what this molecule is. From the modelling point of view, it would be straightforward to add an equation for the rate of change of SIF, and to assume that the differentiation rate (either f in model A, or D in model C) was a function of SIF rather than trypanosome concentration. This would involve addition of extra parameters, the values of which are not known (e.g. rate of SIF secretion, rate of SIF breakdown in the bloodstream and sensitivity of trypanosome differentiation to SIF concentration). Because we have no measurements of SIF concentration as a function of time, we do not have data from which to estimate these parameters and so have not pursued this line in the present paper. Assuming that the half-life of SIF is short, SIF concentration will be approximately proportional to the trypanosome concentration and differentiation rate will be a function of trypanosome concentration.

If a SIF molecule is present, we might ask whether slender and stumpy cells produce it equally. To initiate increased differentiation rate, slender cells must produce SIF, but whether stumpy cells also produce it is less important. Let us consider a modification of model A that assumes that only slender cells produce SIF, and therefore that the differentiation rate $f=f_0X$, instead of equation (3.2). This can be substituted into equation (3.1a) to give

$$\mathrm{d}X/\mathrm{d}t = rX - f_0X^2. \tag{3.7}$$

The diaphorase-negative (slender) concentration is now decoupled from the diaphorase-positive (intermediate and stumpy) concentration. Equation (3.7) is the standard logistic growth equation (Renshaw 1991). According to this, the slender trypanosome concentration would increase towards a stable equilibrium value at $X=r/f_0$, i.e. the differentiation rate would rise to a value sufficient to prevent further increase of slender cells, but insufficient to cause them to decrease. Thus, equation (3.7) cannot explain the observation that the slender population actually passes through a maximum and then decreases. From this we might conclude that the differentiation rate depends on the total trypanosome concentration, not just on the slender cell concentration. This conclusion is weak, however, because if SIF had a longer lifetime, then its concentration would not simply be proportional to X, even if only slender cells produce SIF. Therefore, X would not decouple from other variables, and equation (3.7) would not be valid. Also, we have not yet accounted for the immune system. One could argue that the onset of differentiation merely suffices to prevent further increase of slender cells, whereas the observed decrease is due to the onset of an immune response. Such a scenario might

be advantageous in terms of natural selection as it would favour the maintenance of pleomorphism and, hence, a mix of proliferative forms, which propagate the infection in the mammal, and stumpy forms, which promote transmission through the vector. In view of all these uncertainties, the available data are insufficient to say whether differentiation depends on total trypanosome concentration or only on slender-form trypanosome concentration.

(c) *Addition of the immune response*

Until now, we have tried to explain the decrease in trypanosome concentration in terms of the slender-to-stumpy differentiation and subsequent mortality of stumpy cells. In reality, we know that the host immune response takes an active role in clearing trypanosomes from the bloodstream. Models of the immune system have been proposed in which antibody concentration and/or B-cell concentration are considered as variables with their own differential equations (e.g. Agur *et al.* 1989; Antia *et al.* 1996). We prefer not to do this because we have no direct measurement of antibody concentration over time with which to fit the theoretical curve. We will model the immune response in a very simple way. The essential feature is that the immune response takes time to be activated, i.e. it is zero at the onset of the infection and then rises to a significant level after the host has responded to the presence of trypanosome antigens. Let k be the rate at which trypanosomes are removed by the immune system. We suppose that k is a function of time t since the onset of infection,

$$k = \frac{k_{\max}\exp(t - t_{\mathrm{imm}})}{1 + \exp(t - t_{\mathrm{imm}})}, \tag{3.8}$$

where t_{imm} is the time required for the immune system to respond, and $k_{\max}$ is the maximum rate of trypanosome removal once the immune system is fully activated. This is a sigmoidal function, corresponding to a gradual 'switiching on' of the immune system at time t_{imm}. We now consider model AI (i.e. model A with the addition of the immune response):

$$\mathrm{d}X/\mathrm{d}t = (r - f)X(t) - kX(t), \tag{3.9a}$$

$$\mathrm{d}Y/\mathrm{d}t = fX(t) - kY(t). \tag{3.9b}$$

We suppose, for simplicity, that slender and stumpy cells are killed by the immune system at an equal rate, k. Some experimental evidence indicates that slender cells might be more rapidly removed than stumpy cells (McLintock *et al.* 1993). We have not included this feature as it would involve additional parameters. Also, to keep the number of parameters to a minimum, we have assumed that the rate of immune-mediated stumpy death is greater than the intrinsic mortality rate of stumpy forms. For this reason, the $-mY$ term in equation (3.1b) has been neglected in equation (3.9b), and replaced by the $-kY$ term. The treatment of trypanosome differentiation in this model is as in model A (equation (3.2)), but now both trypanosome differentiation and the immune system limit the parasitaemia.

The fit of mouse 1 data to model AI is shown in figure 5. This is a significant improvement over figure 3, because the fit to T and Y around the maximum is closer

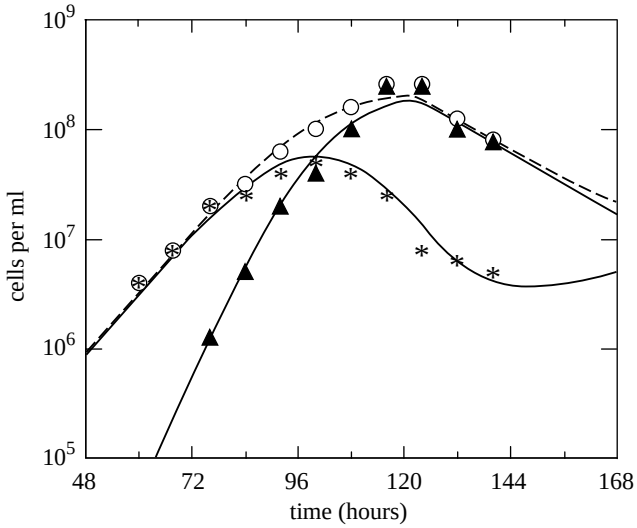

Figure 5. Fit of model AI to the mouse 1 data. Inclusion of both the immune response and the trypanosome differentiation gives a significant improvement of the fit. Parameter values are the same as in figure 3.

and the descent after the maximum is more rapid. Intuitively, this is what we would expect, because the immune system activates when trypanosomes reach high concentration. The rms error is $S = 0.297$, which is the best fit of any of the models considered in this paper. The optimal values of the other parameters are $r = 0.11\,\mathrm{h}^{-1}$; $f_0 = 9.5 \times 10^{-10}\,\mathrm{ml\,h}^{-1}$; $k_{\max} = 0.059\,\mathrm{h}^{-1}$; $t_{\mathrm{imm}} = 122\,\mathrm{h}$; $T_0 = 5.4 \times 10^3\,\mathrm{ml}^{-1}$.

We have also considered addition of the immune response to model C (the obligatory differentiation division model). This gave a fit that was better than model C, however it was worse than model AI, so we will not give the details. These results confirmed that inclusion of both density-dependent differentiation and the immune response gave a better fit to the data than the density-dependent differentiation mechanism alone. We therefore wished to check that the immune response alone did not suffice to fit the data. We did this using equations (3.8), (3.9a) and (3.9b), but we set the differentiation rate f to be a constant parameter, rather than a density-dependent function as in equation (3.2). The best-fit value of the rms error was $S = 1.20$ (shown in figure 6). This is a much worse fit than the other models considered.

The reason for the poor fit in figure 6 can be understood by considering the cell densities during the initial period of exponential growth. In this period, the slender cell density is $X(t)X_0\mathrm{e}^{rt}$. Thus, from equation (3.1b) the stumpy cell concentration satisfies

$$\mathrm{d}Y/\mathrm{d}t = fX_0\mathrm{e}^{rt} - mY. \tag{3.10}$$

If f is constant, as for the model with the immune system only, then the solution is

$$Y(t) \approx (fX_0)/(r + m)(\mathrm{e}^{rt} - \mathrm{e}^{-mt}). \tag{3.11}$$

When $mt \gg 1$, this is just a single exponential increase. Thus, both X and Y increase exponentially at the same rate, which gives parallel lines on the log plot in figure 6. This model therefore cannot explain the fact that the stumpy cells increase more rapidly than the slender

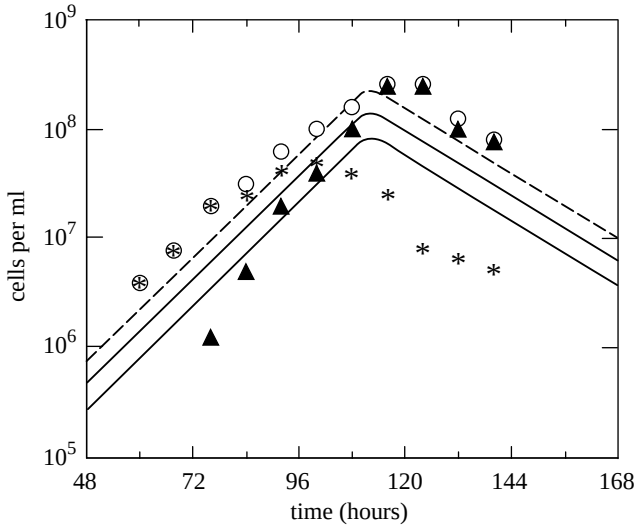

Figure 6. Fitting a model that includes the immune response without density-dependent cell differentiation gives a poor fit, and cannot explain the fact that the curves for the two types of cells cross over each other. Parameter values are the same as in figure 3.

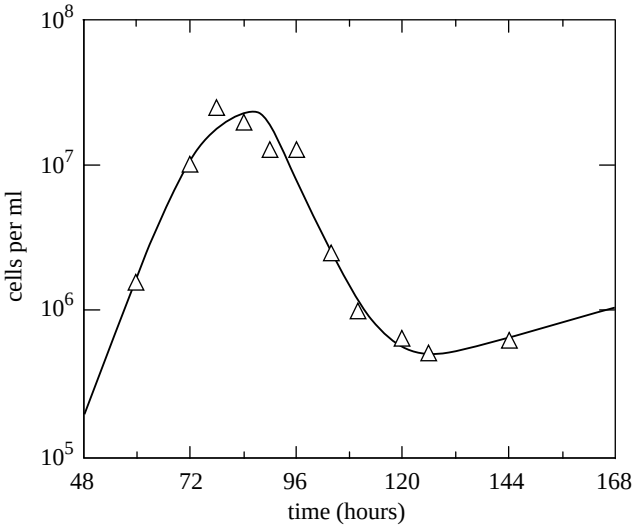

Figure 7. Fitting model AI to the total trypanosome concentration only for one example of a CD1 mouse (taken from figure 1*b*).

cells and eventually become more numerous. Conversely, if $f = f_0 T$, as in the models with density-controlled differentiation, then in the exponential growth phase $f \approx f_0 X$ because almost all cells are slender. Hence,

$$\begin{aligned} \mathrm{d}Y/\mathrm{d}t &= f_0 X_0^2 \mathrm{e}^{2rt} - mY, \\ Y(t) &= ((f_0 X_0^2)/(2r+m))(\mathrm{e}^{2rt} - \mathrm{e}^{-mt}). \end{aligned} \tag{3.12}$$

Thus, the stumpy cells increase exponentially at twice the rate of the slender cells. This is why the curve for Y eventually catches up and overtakes the curve for X.

We have focused on fitting the data from the BALB/c mice with the GUP 2962 trypanosomes, the only system for which independent measurements of the slender and stumpy cell concentrations are available. However, measurements of the total cell concentrations have been made on other systems (as shown above in figure 1). We have tested our preferred theoretical model—model AI—on more limited datasets from another host species (the rat, not shown), and figure 7 shows one example with a CD1 mouse (taken from figure 1*b*). The fit is good and provides an example that the AI model can give rise to other possible shapes of parasitaemia curves.

4. CONCLUSIONS

The parasitaemic profile of *T. brucei* infections is best explained by model AI, in which both density-dependent trypanosome differentiation and host immune response have a role in limiting the increase of parasites. The simpler model A, which incorporates only density-dependent differentiation, gives a qualitative explanation of our data, but a poorer quantitative fit. A model including the immune response, but in which the differentiation rate is not density dependent, gives a very poor fit to the data. These models also make the prediction that the density-dependent trypanosome differentiation mechanism can give rise to oscillations in parasitaemia level. These oscillations are independent of the immune system and are not due to antigenic variation.

Our modelling work also highlights several questions that are biologically important, but for which there is insufficient information in the current data to draw conclusions. First, models of cell-cycle-independent differentiation seem to fit the data better than one of an obligatory differentiation division; however, models that describe these processes are very similar, and in our view, the present data do not allow us to make a firm distinction between the two. Second, the details of the way in which the density-dependent mechanism works remain unclear. Do trypanosomes sense total trypanosome concentration or just slender cell concentration? Is there a SIF molecule, and if so, is it produced by both types of cell or just slender cells? The treatments of the density dependence and the immune response have been deliberately kept as simple as possible, but could be made more precise if suitable data were available for testing the models. Further experimental evidence that might shed light on these points would be of interest.

Programme and equipment grants to K.G. were from the Wellcome Trust. K.M.T. was supported by a BBSRC fellowship.

REFERENCES

Agur, Z., Abiri, D. & Van der Ploeg, L. H. T. 1989 Ordered appearance of antigenic variants of African trypanosomes explained in a mathematical model based on a stochastic switch process and immune-selection against putative switch intermediates. *Proc. Natl Acad. Sci. USA* **86**, 9626–9630.

Antia, R., Nowak, M. A. & Anderson, R. M. 1996 Antigenic variation and the within-host dynamics of parasites. *Proc. Natl Acad. Sci. USA* **93**, 985–989.

Balber, A. 1972 *Trypanosoma brucei*: fluxes of the morphological variants in intact and X-irradiated mice. *Exp. Parasitol.* **31**, 307–319.

Barry, J. D. & Turner, C. M. R. 1991 The dynamics of antigenic variation and growth of African trypanosomes. *Parasitol. Today* **7**, 207–211.

Barry, J. D., Crowe, J. S. & Vickerman, K. 1985 Neutralization of individual variable antigen types in metacyclic populations of *Trypanosoma brucei* does not prevent their subsequent expression in mice. *Parasitology* **90**, 79–88.

Black, S. J., Jack, R. M. & Morrison, W. I. 1983 Host–parasite interactions which influence the virulence of *Trypanosoma* (Trypanozoon) *brucei brucei* organisms. *Acta Trop.* **40**, 11–18.

Black, S. J., Sendashonga, C. N., O'Brien, C., Borowy, M., Naessens, P., Webster, P. & Murray, M. 1985 Regulation of parasitaemia in mice infected with *Trypanosoma brucei*. *Curr. Top. Microbiol. Immunol.* **117**, 93–118.

Frank, S. A. 1999 A model for the sequential dominance of antigenic variants in African trypanosome infections. *Proc. R. Soc. Lond.* B **266**, 1397–1401.

Hamm, B., Schindler, A., Mecke, D. & Duszenko, M. 1990 Differentiation of *Trypanosoma brucei* bloodstream trypomastigotes from long slender to short stumpy forms in axenic culture. *Mol. Biochem. Parasitol.* **40**, 13–22.

Hesse, F., Selzer, P. M., Muhlstadt, K. & Duszenko, M. 1995 A novel cultivation technique for long-term maintenance of bloodstream form trypanosomes *in vitro*. *Mol. Biochem. Parasitol.* **70**, 157–166.

Matthews, K. R. 1999 Developments in the differentiation of *Trypanosoma brucei*. *Parasitol. Today* **15**, 76–80.

Matthews, K. R. & Gull, K. 1994 Evidence for an interplay between cell cycle progression and the initiation of differentiation between life cycle forms of African trypanosomes. *J. Cell Biol.* **125**, 1147–1156.

McLintock, L. M., Turner, C. M. & Vickerman, K. 1990 A comparison of multiplication rates in primary and challenge infections of *Trypanosoma brucei* bloodstream forms. *Parasitology* **101**, 49–55.

McLintock, L. M., Turner, C. M. & Vickerman, K. 1993 Comparison of the effects of immune killing mechanisms on *Trypanosoma brucei* parasites of slender and stumpy morphology. *Parasite Immunol.* **15**, 475–480.

Press, W. H., Teukolsky, S. A., Vetterling, W. T. & Flannery, B. P. 1992 *Numerical recipes in C*, 2nd edn. Cambridge University Press.

Renshaw, E. 1991 *Modelling biological populations in space and time*. Cambridge Studies in Mathematical Biology Series. Cambridge University Press.

Reuner, B., Vassella, E., Yutzy, B. & Boshart, M. 1997 Cell density triggers slender to stumpy differentiation of *Trypanosoma brucei* bloodstream forms in culture. *Mol. Biochem. Parasitol.* **90**, 269–280.

Seed, J. R. & Black, S. J. 1997 A proposed density-dependent model of long slender to short stumpy transformation in the African trypanosomes. *J. Parasitol.* **83**, 6–662.

Seed, J. R. & Black, S. J. 1999 A revised arithmetic model of long slender to short stumpy transformation in the African trypanosomes. *J. Parasitol.* **85**, 850–854.

Seed, J. R. & Sechelski, J. B. 1988 Growth of pleomorphic *Trypanosoma brucei rhodesiense* in irradiated inbred mice. *J. Parasitol.* **74**, 781–789.

Seed, J. R. & Sechelski, J. B. 1989 Mechanism of long slender (LS) to short stumpy (SS) transformation in the African trypanosomes. *J. Protozool.* **36**, 572–577.

Seed, J. R. & Sechelski, J. B. 1995 The inheritance of factors controlling resistance in mice infected with *Trypanosoma brucei rhodesiense*. *J. Parasitol.* **81**, 653–657.

Sendashonga, C. N. & Black, S. J. 1982 Humoral responses against *Trypanosoma brucei* variable surface antigen are induced by degenerating parasites. *Parasite Immunol.* **4**, 245–257.

Turner, C. M. R., Aslam, N. & Dye, C. 1995 Replication, differentiation, growth and the virulence of *Trypanosoma brucei* infections. *Parasitology* **111**, 289–300.

Tyler, K. M. 1998 Differentiation and division of *Trypanosoma brucei* in the mammalian bloodstream. PhD thesis, University of Manchester, UK.

Tyler, K. M., Matthews, K. R. & Gull, K. 1997 The bloodstream differentiation division of *Trypanosoma brucei* studied using mitochondrial markers. *Proc. R. Soc. Lond.* B **264**, 1481–1490.

Tyler, K. M., Matthews, K. R. & Gull, K. 2001 Anisomorphic cell division by African trypanosomes. *Protist*. (In the press.)

Vassella, E. & Boshart, M. 1996 High molecular mass agarose matrix supports growth of bloodstream forms of pleomorphic *Trypanosoma brucei* strains in axenic culture. *Mol. Biochem. Parasitol.* **82**, 91–105.

Vassella, E., Reuner, B., Yutzy, B. & Boshart, M. 1997 Differentiation of African trypanosomes is controlled by a density sensing mechanism which signals cell cycle arrest via the cAMP pathway. *J. Cell Sci.* **110**, 2683–2690.

Vickerman, K. 1965 Polymorphism and mitochondrial activity in sleeping sickness trypanosomes. *Nature* **208**, 762–766.

As this paper exceeds the maximum length normally permitted, the authors have agreed to contribute to production costs.